

30% external quantum efficiency from surface textured, thin-film light-emitting diodes

I. Schnitzer and E. Yablonovitch

UCLA Electrical Engineering Department, University of California, Los Angeles, California 90024-1594

C. Caneau, T. J. Gmitter, and A. Scherer^{a)}

Bellcore, 331 Newman Springs Rd., Red Bank, New Jersey 07701-7040

(Received 9 April 1993; accepted for publication 9 August 1993)

There is a significant gap between the internal efficiency of light-emitting diodes (LEDs) and their external efficiency. The reason for this shortfall is the narrow escape cone for light in high refractive index semiconductors. We have found that by separating thin-film LEDs from their substrates (by epitaxial lift-off, for example), it is much easier for light to escape from the LED structure and thereby avoid absorption. Moreover, by nanotexturing the thin-film surface using "natural lithography," the light ray dynamics becomes chaotic, and the optical phase-space distribution becomes "ergodic," allowing even more of the light to find the escape cone. We have demonstrated 30% external efficiency in GaAs LEDs employing these principles.

High efficiency light-emitting diodes (LEDs) are desired for many applications such as displays, printers, short-haul communications, and optoelectronic computer interconnects. However, there is a significant gap between the internal efficiency of LEDs and their external efficiency. The internal quantum yield of good quality double heterostructures¹ can exceed 99%, as we have demonstrated recently.² On the other hand ordinary LEDs are usually only a few percent efficient. The reason for this shortfall is the difficulty for light to escape from high refractive index semiconductors. The escape cone for internal light in a semiconductor of refractive index $n_s=3.5$ is only $\sim 16^\circ$, as imposed by Snell's Law. This narrow escape cone for spontaneous emission covers a solid angle of $\approx (1/4n_s^2) \times 4\pi$ sr. A mere 2% of the internally generated light can escape into free space, the rest suffering total internal reflection and risking reabsorption.

A number of schemes have partially overcome this problem, based on the old idea³ of coupling the light out of the semiconductor by means of a high refractive index hemispherical dome. Optimally, the hemispherical lens material should be index matched to the semiconductor refractive index. Failing that, the output coupling efficiency will be substantially diminished: $\sim (n_l^2/4n_s^2)$, where n_l is the refractive index of the lens. (For simplicity, n_l is assumed $\ll n_s$.) This formula is actually a general upper limit since it can be derived by statistical mechanical phase-space arguments⁴ without reference to a specific lens geometry. Therefore it applies to inverse Winston concentrators and other types of optical schemes. For a matching refractive index, the "lens" structure needs to be a thick, transparent, semiconductor layer⁵ which can add to the cost. The present state-of-the-art⁶ is $\sim 30\%$ external efficiency in AlGaAs-based LEDs, employing a thick transparent semiconductor superstrate, and total substrate etching in a particularly low-loss optical design.

The key to increasing the escape probability is to give the photons multiple opportunities to find the escape cone. In other words there should be an efficient mechanism that

redirects photons which were originally emitted out of the escape cone, back into the escape cone. Chaotic photon trajectories lead to an *ergodic* distribution of light in which the time-average photon trajectories are equivalent to a phase-space average. This assures the maximum statistically feasible output coupling from the LED through the escape cone.

One way to mix angles is by photon reabsorption and re-emission, but this requires extremely good material quality and low parasitic absorption. In Ref. 2 we used the epitaxial lift-off (ELO) technique⁷ to mount thin-film heterostructures onto high reflectivity surfaces, as shown in Fig. 1(a). Photon recycling, implemented with high quality material (internal quantum yield of $\eta \approx 99.7\%$), produced an impressive external quantum efficiency of $\eta_{\text{ext}} = 72\%$ from the optically pumped double heterostructure. However, it was also demonstrated that this high external efficiency is very susceptible to parasitic loss mechanisms (free-carrier absorption in doped layers, for example) or slight degradation in the internal quantum efficiency. Angular randomization by photon recycling is not practical since it is vulnerable to the slightest deterioration of material or mirror quality. A more practical approach, and the one which we adopt here, is angular randomization by scattering of the photons from textured semiconductor sur-

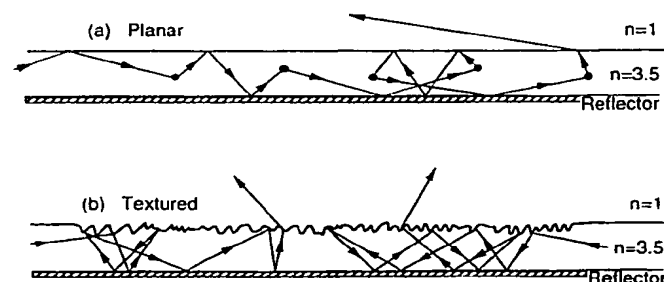


FIG. 1. Typical photon trajectories in the thin epi-lift-off heterostructures: (a) In the planar structure, photons' trajectories are randomized by self-absorption/re-emission events represented by dots (photons recycling). (b) In the textured film, angular randomization is achieved by strong surface scattering.

^{a)}Present address: Caltech, Pasadena, CA 91125.

faces. Thus the textured film geometry, schematically shown in Fig. 1(b), can boost the external efficiency to 50% or more, while relieving the demand for (i), the utmost material quality and (ii), low parasitic losses, as required by the planar film geometry of Fig. 1(a).

Our approach has two key components: (i) separation of thin-film heterojunctions from the growth substrate using the ELO⁷ technique, and (ii) nanotexturing of the thin-film semiconductor surface by natural lithography.⁸ The principles and the device geometry that are demonstrated here can be applied to other material systems to obtain bright visible LEDs as well.

To model the behavior of the trapped photons we invoke a rate equation approach which was introduced⁴ to analyze the ergodic behavior of light in solar cells and LEDs. The implicit assumption of such an approach is that the photon trajectories are completely randomized with respect to internal angles in the semiconductor, i.e., they behave as a photon gas. In steady state, the photon creation rate and total loss rate balance. Hence the external efficiency is given by the ratio of the emission rate into the escape cone, to the total loss rate.

In general, photons will be lost from the semiconductor by escape through the film's top surface, and by absorption in the bulk and at the rear reflector surface. The loss rate by escape through the top surface is:

$$\int_0^{\theta_c} \int dA B_{\text{int}} T(\theta) \cos \theta 2\pi \sin \theta d\theta = \frac{\pi B_{\text{int}} A \bar{T}}{n^2}, \quad (1)$$

where B_{int} is the internal brightness in photons/cm²/s/sr, θ is the polar angle, A is the surface area, θ_c is the critical escape angle ($\sim 16^\circ$) given by $\sin \theta_c = 1/n$, and \bar{T} is the angle averaged transmission coefficient through the top semiconductor surface. The loss rate due to absorption at the rear reflector surface is also a surface integral

$$\int \int_0^{\pi/2} dA B_{\text{int}} [1 - R(\theta)] \cos \theta 2\pi \sin \theta d\theta = \pi B_{\text{int}} A [1 - \bar{R}] \quad (2)$$

and \bar{R} is the angle averaged reflectivity. The loss of photons from the bulk is given by the volume integrated absorption

$$\int \alpha(z) B_{\text{int}} d\Omega dV = 4\pi B_{\text{int}} A \left((1 - \eta) \alpha_0 d_0 + \sum_{j \neq 0} \alpha_j d_j \right), \quad (3)$$

where dV is the volume increment, $d\Omega$ is the solid-angle increment, $\alpha(z)$ is the local absorption coefficient, and α_j and d_j are the absorptivity and thickness of the j th layer, respectively. The band-to-band absorption in the active layer, α_0 , produces electron-hole pairs, which may be subdivided into a portion $(1 - \eta) \alpha_0$, which leads to nonradiative recombination and heat, and a portion $\eta \alpha_0$ which leads to radiative re-emission. The radiative part rejoins the internal photon gas with no net loss or gain and is not included in the rate equations. By contrast, parasitic absorption in the layers $j \neq 0$, is regarded as a total loss.

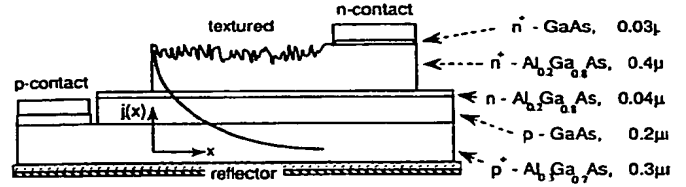


FIG. 2. Schematic cross section of an epi-lift-off, textured, LED van der Waals bonded onto a SiO₂ coated metallic reflector. The narrow spatial distribution of injection current [the curve on the graph $j(x)$ vs x] is due to intentional current crowding. This helps keep the light-emitting region away from the absorbing electrical contacts. The width of the textured stripe is ~ 50 times the film thickness.

The escape efficiency is given by the ratio between the outflow through the escape cone, Eq. (1), divided by the total photon outflow, Eqs. (1)–(3). Hence, the external quantum efficiency of the LED is given by

$$\eta_{\text{ext}} = \eta \frac{\bar{T}/4n^2}{\bar{T}/4n^2 + (1 - \eta) \alpha_0 d_0 + L/4}, \quad (4)$$

where all the parasitic loss terms are included in the double-pass loss $L \equiv (1 - \bar{R}) + \sum \alpha_j d_j$. Thus parasitic losses 0.05 per pass boosts LED efficiency to 50% or more.

The actual LED structure is shown in Fig. 2. A conventional n^+ -AlGaAs/ p -GaAs/ p^+ -AlGaAs double heterostructure is grown over a 0.05-μm-thick AlAs release layer by organometallic chemical vapor deposition. LED arrays are fully processed from these wafers and then tested. The arrays are then separated from the GaAs substrate by ELO,⁶ using HF acid selective etching of the AlAs release layer. Then thin-film arrays, supported from above by a thick wax layer, are van der Waals bonded by surface tension forces⁹ onto large area dielectric coated Au mirrors. These reflecting substrates offer a high angle averaged reflectivity² compared to conventional metallic mirrors, or an epitaxially grown AlAs/GaAs Bragg reflector.¹⁰

To eliminate the strong parasitic absorption at the electrodes, a significant problem in all LEDs, we have employed a LED design which uses lateral injection and depends on current crowding,¹¹ as shown in Fig. 2. The diode current is crowded into a central region between the two ohmic contacts, but reasonably distant from either contact. This minimizes parasitic optical absorption at the ohmic contacts.

In Fig. 2, the GaAs active region is doped with a holes to a moderate density $p = 3 \times 10^{17} \text{ cm}^{-3}$, near the optimum density for good internal luminescence yield. The sheet conductivity of the n^+ -Al_{0.2}Ga_{0.8}As layer is much greater than that of the p^+ -Al_{0.3}Ga_{0.7}As layer due to the difference in mobility of electrons and holes, even though both layers are doped to $3 \times 10^{18} \text{ cm}^{-3}$. Since the n^+ -Al_{0.2}Ga_{0.8}As heterocontact layer extends only part way between electrodes, the electron injection will be forced to occur just before this layer ends. Due to the higher resistance of the p^+ -Al_{0.3}Ga_{0.7}As heterocontact layer, the hole current will not extend far under the edge of the n^+ conductive layer. Thus, resistive voltage drops in the p^+ layer "crowd" the diode

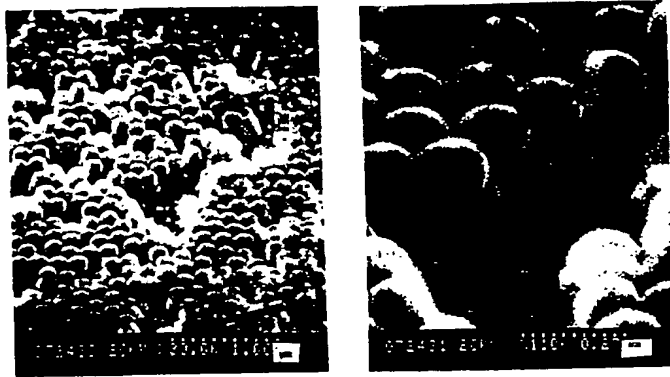


FIG. 3. Natural lithography: Polystyrene spheres, 0.2- μm diam, coat the surface of the LED in a randomly close-packed array. The spheres then act as an etch mask for Cl_2 assisted Xe^+ ion beam etching, about 0.17- μm deep. The high refractive index textured surface permits ergodic phase-space filling of the light waves, which optimizes the external efficiency.

forward current density into a narrow region as indicated by the graph $j(x)$ vs x in Fig. 2.

Edge passivation, a necessity for minority carrier devices, is provided by the extension of the p -GaAs active layer past the n^+ - $\text{Al}_{0.2}\text{Ga}_{0.8}\text{As}$ contact step. The p -GaAs active region extension is passivated on top by the 40 nm n - $\text{Al}_{0.2}\text{Ga}_{0.8}\text{As}$ layer. This layer is thin enough to be depleted, so there is no electron conduction to the exposed p -GaAs edge, which appears as a second step, about 15 μm away from the n^+ contact step. The exposed edge is unpassivated, but far enough away from the pumped region that the diffusive recombination current is negligible. Effectively, the structure in Fig. 2 passivates the exposed edge by means of a 15- μm -wide diffusion barrier.

The final processing step is "natural lithography" on the light-emitting region which takes place after thin-film transfer and bonding. Experiments have shown¹² that a surface texture on a scale of half an internal optical wavelength will produce complete internal angular randomization of light rays in a semiconductor film. A scanning electron micrograph of the surface texture produced by natural lithography is shown in Fig. 3. Polystyrene spheres, 0.2- μm diam, coat the surface of the LED in a randomly close-packed array. The polystyrene spheres are attached by surface forces in a dipping process or by spin coating from aqueous solution. The spheres then act as an etch mask for a Cl_2 assisted Xe^+ ion beam etching,¹³ about 0.17 μm deep into the n^+ - $\text{Al}_{0.2}\text{Ga}_{0.8}\text{As}$ layer.

Total LED light emission vs the injection current is plotted in Fig. 4. Absolute calibration is obtained by the ratio of photodiode current to LED current, with a small correction for photodiode quantum efficiency. The angular distribution of light from these LEDs is Lambertian. The linear fits on Fig. 4 indicate the broad optimal current range, which is limited by heating at the high end and nonradiative recombination at the low end. The squares and diamonds represent two devices drawn from the same wafer and processed together up to the final texturing step. In both cases a significant portion of the photon gas dif-

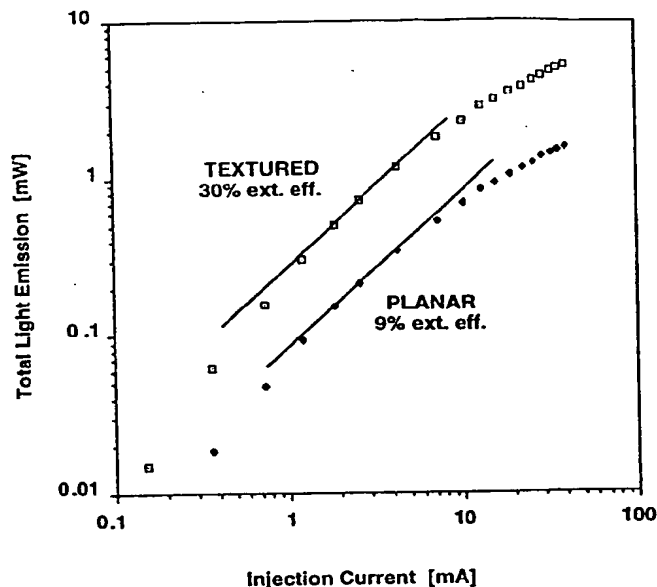


FIG. 4. Log-log plot of the measured total light output vs injection current, for typical textured and planar LEDs.

fuses towards the planar section near the p contact, which somewhat diminishes the performance of this structure. We have modeled the results in Fig. 4 and concluded that the efficiency was limited both by material quality and device geometry, and that further improvements are feasible.

LEDs are simpler and more reliable than lasers. Unlike lasers they do not require a threshold current, yet they may compete with laser diode efficiency. It is clear that the availability of 30%–50% efficient, visible LEDs would be quite useful. The authors thank H. W. Deckman, S. A. Schwarz of DARPA and ONR under Contract No. N0014-93-1-0311.

¹R. J. Nelson and R. G. Sobers, *J. Appl. Phys.* **49**, 6103 (1978).

²I. Schnitzer, E. Yablonovitch, C. Caneau, and T. J. Gmitter, *Appl. Phys. Lett.* **62**, 131 (1993).

³W. N. Carr and G. E. Pittman, *Appl. Phys. Lett.* **3**, 173 (1963).

⁴E. Yablonovitch, *J. Opt. Soc. Am.* **72**, 899 (1982); E. Yablonovitch and G. D. Cody, *IEEE Trans. Electron. Devices* **ED-29**, 300 (1982); W. B. Joyce, R. Z. Bachrach, R. W. Dixon, and D. A. Sealer, *J. Appl. Phys.* **45**, 2229 (1974).

⁵K. H. Huang, J. G. Yu, C. P. Kuo, R. M. Fletcher, T. D. Osentowski, L. J. Stinson, M. G. Craford, and A. S. H. Liao, *Appl. Phys. Lett.* **61**, 1045 (1992); C. P. Kuo, R. M. Fletcher, T. D. Osentowski, M. C. Lardizabal, M. G. Craford, and V. M. Robbins, *ibid.* **57**, 2937 (1990).

⁶M. G. Craford, oral presentation 51st Device Research Conference, Santa Barbara, CA, 1993 (unpublished).

⁷E. Yablonovitch, T. J. Gmitter, J. P. Harbison, and R. Bhat, *Appl. Phys. Lett.* **51**, 2222 (1987).

⁸H. W. Deckman and J. H. Dunsmuir, *Appl. Phys. Lett.* **41**, 377 (1982).

⁹E. Yablonovitch, D. M. Hwang, T. J. Gmitter, L. T. Florez and J. P. Harbison, *Appl. Phys. Lett.* **56**, 2419 (1990).

¹⁰E. F. Schubert, Y.-H. Wang, A. Y. Cho, L.-W. Tu, and G. J. Zydzik, *Appl. Phys. Lett.* **60**, 921 (1992); N. E. J. Hunt, E. F. Schubert, R. A. Logan, and G. J. Zydzik, *ibid.* **61**, 2287 (1992).

¹¹W. B. Joyce and S. H. Wemple, *J. Appl. Phys.* **41**, 3818 (1970).

¹²H. W. Deckman, C. B. Roxlo, and E. Yablonovitch, *Opt. Lett.* **8**, 491 (1983); H. W. Deckman, C. R. Wronski, H. Witzke, and E. Yablonovitch, *Appl. Phys. Lett.* **42**, 968 (1983).

¹³A. Scherer and B. P. Van der Gaag, *Proc. SPIE* **1284**, 149, 161 (1990).

THIS PAGE BLANK (USPTO)